Published in final edited form as:
Endocrinology. 2005 November ; 146(11): 4647–4656. doi:10.1210/en.2005-0670.

Analysis of the Biochemical Mechanisms for the Endocrine Actions of Fibroblast Growth Factor-23

Xijie Yu, **Omar A. Ibrahimi**, **Regina Goetz**, **Fuming Zhang**, **Siobhan I. Davis**, **Holly J. Garringer**, **Robert J. Linhardt**, **David M. Ornitz**, **Moosa Mohammadi**, and **Kenneth E. White**
Department of Medical & Molecular Genetics (X.Y., S.I.D., H.J.G., K.E.W.), Indiana University School of Medicine, Indianapolis, Indiana 46202; Department of Pharmacology (O.A.I., R.G., M.M.), New York University School of Medicine, New York, New York 10016; Department of Chemistry & Chemical Biology (F.Z., R.J.L.), Rensselaer Polytechnic Institute, Troy, New York 12180; and Department of Molecular Biology and Pharmacology (D.M.O.), Washington University Medical School, St. Louis, Missouri 63110

Abstract

Fibroblast growth factor (FGF)-23 has emerged as an endocrine regulator of phosphate and of vitamin D metabolism. It is produced in bone and, unlike other FGFs, circulates in the bloodstream to ultimately regulate phosphate handling and vitamin D production in the kidney. Presently, it is unknown which of the seven principal FGF receptors (FGFRs) transmits FGF23 biological activity. Furthermore, the molecular basis for the endocrine mode of FGF23 action is unclear. Herein, we performed surface plasmon resonance and mitogenesis experiments to comprehensively characterize receptor binding specificity. Our data demonstrate that FGF23 binds and activates the c splice isoforms of FGFR1-3, as well as FGFR4, but not the b splice isoforms of FGFR1-3. Interestingly, highly sulfated and longer glycosaminoglycan (GAG) species were capable of promoting FGF23 mitogenic activity. We also show that FGF23 induces tyrosine phosphorylation and inhibits sodium-phosphate cotransporter Npt2a mRNA expression using opossum kidney cells, a model kidney proximal tubule cell line. Removal of cell surface GAGs abolishes the effects of FGF23, and exogenous highly sulfated GAG is capable of restoring FGF23 activity, suggesting that proximal tubule cells naturally express GAGs that are permissive for FGF23 action. We propose that FGF23 signals through multiple FGFRs and that the unique endocrine actions of FGF23 involve escape from FGF23-producing cells and circulation to the kidney, where highly sulfated GAGs most likely act as cofactors for FGF23 activity. Our biochemical findings provide important insights into the molecular mechanisms by which dysregulated FGF23 signaling leads to disorders of hyper- and hypophosphatemia.

The fibroblast growth factor (FGF) family of ligands plays fundamental roles in development as well as in basic metabolic processes. The cellular effects of FGFs are mediated by FGF receptor (FGFR) tyrosine kinases that are encoded by four distinct genes (FGFR1-4) in mammals. The prototypic FGFR consists of three extracellular Ig-like

Address all correspondence and requests for reprints to: Kenneth E. White, Ph.D., 975 West Walnut Street, IB130, Indiana University School of Medicine, Indianapolis, Indiana 46202. kenewhit@iupui.edu.

domains (D1–D3), a single transmembrane domain, and an intracellular tyrosine kinase domain (reviewed in Ref. 1). A major alternative splicing occurs within D3 of FGFR1-3, resulting in b and c receptor isoforms that exhibit distinct ligand binding specificities (2, 3). Receptor dimerization is a mandatory event in FGF signalingand,inadditiontothe FGF ligand, requires the presence of heparin/heparan sulfate (HS) polysaccharide chains of HS proteoglycans. Importantly, expression patterns of heparin/HS undergo dynamic changes during normal development to provide differential FGF signaling within tissues (4).

FGF23 is central to the regulation of phosphate and vitamin D metabolism, as evidenced by the fact that mutations in FGF23 result in the metabolic bone disorder autosomal dominant hypophosphatemic rickets (ADHR) (5). Missense mutations involving the arginine residues within the $_{176}RXXR_{179}/S_{180}$ motif are thought to stabilize full-length FGF23 in ADHR through resistance to furin-like intracellular protease cleavage (6, 7). Although most FGFs are paracrine and autocrine factors, FGF23 uniquely acts as an endocrine factor. Unlike other FGFs, FGF23 can be detected in normal serum and, additionally, circulating FGF23 concentrations are elevated in many X-linked hypophosphatemia (XLH), tumor-induced osteomalacia (TIO), and fibrous dysplasia patients, who share similar phenotypes with ADHR patients (8–10). Of significance, we and others have shown that recessive FGF23 missense mutations that lead to decreased plasma levels of intact FGF23 protein cause familial tumoral calcinosis, a disorder of hyperphosphatemia coincident with elevated circulating 1,25-dihydroxyvitamin D concentrations (11, 12). Recent studies further indicate that there is an inverse relationship between serum FGF23 and phosphate levels in humans (13).

Genetic manipulations in mice support the idea that excessive circulating FGF23 contributes to the etiology of human phosphate wasting disorders. In this regard, FGF23 transgenic mice are phenocopies for the clinical features of ADHR, TIO, and XLH, including hypophosphatemia due to renal phosphate wasting, inappropriately low serum 1,25-dihydroxyvitamin D levels, and rachitic bone (14–16). Furthermore, administration of either recombinant wild-type FGF23 or FGF23 harboring the ADHR mutations induces hypophosphatemia in normal mice accompanied by increased renal phosphate excretion (7, 17). Conversely, mice null for Fgf23 display a reciprocal phenotype to ADHR patients and, thus, manifest hyperphosphatemia secondary to increased renal phosphate reabsorption, as well as increased circulating 1,25-dihydroxyvitamin D concentrations (18,19).

Despite mounting genetic and biochemical evidence that FGF23 is a novel phosphaturic hormone, the molecular pathways by which FGF23 regulates phosphate and vitamin D homeostasis are poorly understood. To gain insight into the molecular mechanisms of FGF23 action, we characterized the receptor binding and activation specificity of FGF23 using surface plasmon resonance (SPR) in combination with cell-proliferation studies. Furthermore, we tested the ability of FGF23 and specific glycosaminoglycans (GAGs) to regulate the tyrosine phosphorylation and the expression of the sodium phosphate cotransporter Npt2a in opossum kidney (OK) cells, an *in vitro* model for kidney proximal tubule cells. Together, our data demonstrate that FGF23 interacts with multiple FGFRs and that the stimulation of these receptor isoforms requires highly sulfated GAGs.

Materials and Methods

SPR analyses of FGF23-FGFR interactions

Mature human full-length FGF23 was expressed in *Escherichia coli* and purified by affinity chromatography, ion exchange, and size-exclusion chromatography in a manner similar to our published protocol (20). FGFR isoform ectodomains were prepared without fusion protein tags as previously described (20, 21). FGF23-FGFR interactions were tested using a BIAcore 3000 instrument (Biacore AB, Uppsala, Sweden). Briefly, FGF23 was immobilized on research grade carboxy-methylated 5 chips according to standard amine coupling protocol (Biacore AB). To obtain kinetic data, different concentrations of each FGFR in HBS-EP buffer [0.01 M HEPES, 0.15 M NaCl, 3 mM EDTA, 0.005% polysorbate 20 (vol/ vol), pH 7.4] were injected over the FGF23 sensor chips at a flow rate of 50 μl/min. At the end of each sample injection (180 sec), HBS-EP buffer was passed over the sensor surface to monitor dissociation. After 180 sec of dissociation, the sensor surface was fully regenerated by injection of 50 μl of 2 M NaCl in 100 mM sodium acetate buffer (pH 4.5).

SPR data analysis

Responses from the control flow cell, containing immobilized FHF1b, formerly classified as FGF12, were subtracted from FGF23 flow cells for each set of analyte injections using BiaEvaluation software (Biacore AB). The resulting sensorgrams were used for kinetic parameter determination by globally fitting the entire association and dissociation phases to a 1:1 interaction using BiaEvaluation software (Biacore AB) as previously described (20). After curve fitting, each sensorgram was manually examined for the closeness of the model fit to the experimental data. χ^2 was less than 10% of R_{max} for each fit.

Preparation of GAG analogs and heparins

The fully *O*-sulfated GAGs dermatan sulfate (*O*-DS), chondroitin sulfate (*O*-CS), and hyaluronic acid (*O*-HA) were prepared by chemical sulfonation of DS, CS, and HA, respectively (22–24). The *N*,*O*-sulfated heparin (*N*,*O*-SH) was prepared by *O*-sulfonation followed by *N*-sulfonation of heparin, as previously described (23, 24). Heparin oligosaccharides of defined degree of polymerization (dp) were prepared from controlled partial heparin lyase 1 treatment of bovine heparin followed by size fractionation as described (25,26). Highly purified low molecular weight heparin sodium salt, heparin from porcine intestine, and crude, unbleached heparin sodium salt containing GAG heparin 90% and peptidoglycan heparin 10%, and heparin monosulfate (HS-M) were purchased from Sigma-Aldrich (St. Louis, MO).

BaF3 proliferation assays

The BaF3 cell lines ectopically expressing the major FGFR splice variants have been previously described (3). These cell lines were engineered to express each of the three Ig-like domain, b and c splice forms, of FGFR1-3, or the two Ig-like domain form of FGFR4, by electroporating with FGFR plasmids and selecting in media containing G418 to obtain stable BaF3 cell lines expressing the individual FGFRs. Analysis of the FGFR-expressing BaF3 cell lines, by cross-linking of cell surface receptors to labeled FGF1 or by Western

blotting, demonstrated that all cell lines express comparable levels of cell surface receptor (3). These BaF3-FGFR cell lines were maintained in RPMI 1640 media (Sigma) supplemented with 10% fetal bovine serum (FBS), 0.5 ng/ml IL-3 (PeproTech, Inc., Rocky Hill, NJ), 2 mM L-glutamine, penicillin (50 IU/ml) and streptomycin (50 μg/ml), and 50 nM β-mercaptoethanol. Recombinant FGF1 was obtained from R&D Systems, Inc. (Minneapolis, MN). For mitogenic assays, BaF3 cells expressing specific FGFRs (FGFR1b, 1c, 2b, 2c, 3b, 3c, 4) were washed and resuspended in RPMI 1640, 10% FBS, L-glutamine, penicillin and streptomycin, and 50 nM β-mercaptoethanol. Cells (30,000) were plated per well in a 96-well assay plate in media containing 2 μg/ml heparin. FGFs were added to each well for a total volume of 200 μl per well. The cells were then incubated at 37 C for 40 h. To each well, 40 μl of Aqueous One Solution (Promega, Madison, WI) was added, and cells were incubated at 37 C for 4 h. The concentration of the metabolic product formazan, which is directly proportional to cell number, was measured by absorbance at 490 nm.

Cellular tyrosine kinase activity in OK cells

OK cells (OK/E), which possess a proximal tubule cell-like phenotype, were maintained in a humidified incubator at 37 C under 5% CO_2 atmosphere in DMEM/Ham's F-12 medium (1:1), supplemented with 10% FBS, 2 mM L-glutamine, penicillin (50 IU/ml), and streptomycin (50 μg/ml). OK cells, 5000 per well, were cultured in 96-well plate for 24 h Cells were starved with serum-free medium plus 0.2% BSA for 24 h, then treated either with vehicle (PBS), 100 nM PTH, or 100 nM FGF23 with or without 2 μg/ml heparin in serum-free medium plus 0.2% BSA for 15 min. The cellular phosphotyrosine activity was assessed by using an ELISA kit according to the protocol of the manufacturer (RayBiotech, Inc., Norcross, GA). Briefly, the cells were fixed at room temperature for 10 min. After blocking, anti-phosphotyrosine-horseradish peroxidase antibody was added and incubated at room temperature for 1 h. A 3,3',5,5'-tetramethylbenzidine substrate developing solution was added for 30 min; then a stop solution was added to each well, and the intensity of the color was measured by absorbance at 450 nm.

RNA extraction

OK cells were cultured in 12-well plates at a density of 50,000 per well for 24 h. Cells were starved with serum-free medium plus 0.2% BSA for 24 h and then treated either with vehicle (PBS), PTH, or FGF23 with or without heparin at the specified concentrations. To block heparan sulfate (HS) sulfation, sodium chlorate was used. The agent inhibits the generation of 3'-phosphoadenosine 5'-phosphosulfate, the natural donor of sulfate groups necessary for HS sulfation (27, 28). Sodium chlorate at 50 mM was used for all experiments. Cells (25,000 per well) were cultured in 12-well plates and maintained for 24 h. The cells were then treated with sodium chlorate in regular medium for 24 h and starved with serum-free medium plus 0.2% BSA in the presence of 50 mM sodium chlorate for an additional 48 h. Next, the cells were treated with vehicle (PBS), 100 nM PTH, or 100 nM FGF23 with or without 2 μg/ml heparin in serum-free medium plus 0.2% BSA and 50 mM sodium chlorate and maintained for another 24 h RNA was extracted from OK cells using RNeasy Mini kit (Qiagen, Inc., Valencia, CA). On-column DNase digestion was performed with the RNase-Free DNase set (Qiagen Inc.) to remove residual genomic DNA. RNA concentrations were quantified using the Biophotometer spectrophotometer (Eppendorf, Hamburg, Germany).

TaqMan probes and primers

The TaqMan primers and probe for opossum Npt2a and β-actin (Table 1) were designed using Primer Express software (Applied Bio-systems, Foster City, CA). The primers and probe for Npt2a were designed to span at least one intron to eliminate nonspecific signals due to genomic DNA amplification. Because the opossum β-actin has not been fully cloned, β-actin was amplified from OK cell RNA by RT-PCR with primers based upon the mouse sequence: forward, 5'ACAACG-GCTCCGGCATGTGCAA3'; reverse, 5'TACTCCTGCTTGCTGATC-CACA3'. The β-actin cDNA product was sequenced, and TaqMan primers and probe were designed from this template as an internal control (Table 1).

Real-time RT-PCR assays

RT and real-time quantitative PCR were performed in a one-step reaction using the TaqMan Gold RT-PCR kit and protocols provided by the manufacturer (Applied Biosystems). Briefly, a typical reaction contained 50 ng total RNA and 1.25 U of Gold DNA polymerase, 12.5 U of MultiScribe Reverse Transcriptase, and 5.5 mM $MgCl_2$ in a 50-μl reaction volume. Primers and TaqMan probes were added at a final concentration 200 nM and 100 nM, respectively. The dNTP final concentration was 0.3 mM each except for dUTP, which was 0.6 mM. Amplification of Npt2a and the β-actin RNAs was performed in the same plate using the ABI-PRISM 7700 Sequence Detection System (Applied Biosystems). The thermal cycling protocol consisted of RT at 48 C for 30 min and activation of Gold DNA polymerase at 95 C for 5 min, followed by 40 cycles of template denaturing at 95 C for 15 sec and annealing/extension at 60 C for 1 min. Accumulation of the PCR products was detected by directly monitoring the increase in fluorescence of the reporter dye (6-carboxyfluorescein for Npt2a; VIC for β-actin). The mean of the background fluorescence emission for all tested wells measured between cycles 3 and 14 used to set the baseline. A threshold for the amplification of each gene of interest was then established by drawing a line that intersected the exponential phase of the logarithmic amplification curves for all samples being analyzed for the expression of the target gene. All primer sets were tested for specific amplification of mRNA by parallel analyses of controls that included omitting RT or template and resulted in no fluorescent signal detection. Each RNA sample was analyzed in triplicate, and each experiment was performed independently at least three times. The amplification of Npt2a and β-actin was equally efficient, and the $2^{-\Delta\Delta CT}$ method described by Livak and Schmittgen (29) was used to analyze the data. The expression level of Npt2a and β-actin mRNA was calculated relative to no treatment control.

Statistical analysis

Data were analyzed using JMP Statistical Discovery Software 4.1 (SAS Inc., Cary, NC). Statistical analysis of the data were performed by paired Tukey-Kramer honestly significant difference. Statistical significance for all tests was set at $P < 0.05$. Data are presented as means ± SEM.

Results

Receptor-binding specificity of FGF23 in vitro

Presently, it is unknown which of the seven principal FGFRs (FGFR1b, 1c, 2b, 2c, 3b, 3c, and 4) mediates FGF23 activity. Hence, we employed SPR to comprehensively characterize the FGFR binding specificity of FGF23. Recombinant FGF23 was immobilized on biosensor chips, and varying concentrations of each of the seven FGFR ectodomains were injected over these chips. Analysis of the SPR data demonstrated that FGF23 interacts with the c isoforms of FGFR1-3 and FGFR4 with dissociation constants ranging from 200–700 n_M (Fig. 1 and Table 2). FGF23 does not interact significantly with the b isoforms of FGFR1-3 (not shown).

Receptor activation specificity of FGF23 using BaF3 cell lines

BaF3 cells are a murine bone marrow-derived pro-B cell line and have been used extensively to investigate the activity of a variety of receptor tyrosine kinases, including FGFs (3, 30–33). This cell line is dependent up on IL-3 for growth, and this IL-3-dependent growth can be replaced by ligands for receptor tyrosine kinases, when the appropriate receptor is transiently or stably expressed in the BaF3 cell (31). Wildtype BaF3 cells do not express FGFRs or HS proteoglycans (3, 30, 34). Therefore, BaF3 cells stably transfected with FGFR1b, 1c, 2b, 2c, 3b, 3c, and 4 have been treated with exogenous FGFs and heparin and have been shown to proliferate in response to FGFR stimulation (3, 30, 34). Thus, mitogenicity of any individual cell line represents the stimulation of a specific FGFR isoform and receptor tyrosine kinase activity. We used these well-characterized BaF3 cell lines to provide biological evidence for the receptor binding specificity pattern of FGF23 observed in the SPR experiments described above. FGF23, in the presence of sodium heparin (unbleached), specifically activated FGFR1c (235% of control), 2c (243%), 3c (294%), and 4 (318%) (Fig. 2A). FGF23 also activated the receptors in the presence of porcine intestinal mucosal heparin and low-molecular-weight heparin (not shown). In contrast, FGF23 showed negligible activity toward BaF3 cells expressing FGFR1b, 2b, and 3b (Fig. 2A). Either FGF23 or heparin alone did not induce proliferative responses in any cell line. FGF1 is the prototypical paracrine FGF and considered to be the universal FGFR ligand because it can stimulate proliferation of all the seven FGFR-BaF3 cell lines (3). Therefore, we used FGF1 as the positive control in proliferation assays. Consistent with published literature, FGF1 stimulated proliferation of all seven cell lines and was more potent than FGF23 in stimulating the proliferation of the BaF3 cell lines expressing the c isoforms of FGFR1-3 and FGFR4 (Fig. 2B).

FGF23 prefers highly sulfated GAGs to induce biological signals

The endocrine mode of action of FGF23 distinguishes FGF23 from conventional FGFs, such as FGF1, that act locally within tissues. Harmonious with their paracrine mode of action, these conventional FGFs are sequestered by HS in the pericellular environment, not far from the FGF-producing cells for local binding and activation of FGFRs. The fact that FGF23 has modest receptor affinity but endocrine action is intriguing and led us to hypothesize that FGF23 may exhibit preference for subsets of GAGs to produce biological activity in target tissues.

To test our hypothesis, we assayed a library of in-houseprepared GAGs and GAG derivatives for the ability to promote FGF23-mediated proliferation of BaF3 cells expressing FGFR1c. Specifically, we used tissue-purified GAG preparations, including DS, CS, and HA. None of these GAGs was capable of producing a proliferative response in the BaF3-FGFR cell assays (not shown). These results led us to reason that the specific GAGs that confer FGF23 activity in tissue preparations may be expressed in amounts too low to induce significant FGF23 activity. Because GAG sulfation could also be a critical factor in FGF23 stimulation of the FGFRs, we examined the effects of oversulfated GAG species on FGF23 activity. The oversulfated GAGs were *N,O-SH*, *O*-DS, *O*-CS, and *O*-HA. Because FGFR1 has the widest tissue distribution of all FGFRs, we reasoned that this receptor may possess the greatest response profile to a variety of GAGs. Indeed, FGF23 produced a proliferative response using FGFR1c with *N,O*-SH (398% of heparin alone control), *O*-DS (332%), *O*-CS (332%), and *O*-HA (271%) (Fig. 3A; $P < 0.0001$ *vs*. controls). Of note, this proliferative effect in these experiments was 50–70% greater than the effects that we observed using the commercial heparin preparations (Fig. 2). In contrast to the oversulfated GAGs, HS-M was unable to support the mitogenic activity of FGF23 (Fig. 3A).

Oversulfated GAGs, composed of entirely different monosaccharides, promoted FGF23 activity. This suggested that a high degree of sulfation, rather than the type of sugar backbone, determines the biological activity of GAGs in the context of FGF23. To test this hypothesis further, we examined the ability of fully sulfated fucose, xylose, and glucose oligomers not based upon GAG structure to promote FGF23 activity. A fully sulfated β-linked xylose-based hexasaccharide, a branched β-linked glucose-based hexasaccharide, and fully sulfated a-linked fucose-based tetrasaccharide, a linear [1,6]β-linked glucose-based tetrasaccharide, were unable to induce FGF23 activity (Fig. 3A). FGF1 served as the positive control, and significantly stimulated proliferation with most of the polysaccharides as well as with HS-M (Fig. 3B). Sulfated polysaccharides that did not synergize with FGF23 or FGF1 included sulfated fucose tetrasaccharide, a fully sulfated α-linked linear fucose tetrasaccharide, sulfated octyl-3-*O*-methyl xylopranosyl hexasaccharide, a fully sulfated β-linked linear xylopyrranosyl hexasaccharide, and fully sulfated tetrasaccharide (α), a fully sulfated [1,6]β-linked linear glucose tetrasaccharide (not shown). These experiments indicate that charge alone is insufficient for FGF23 activation of FGFRs and that specific backbones, consisting of repeating hexosamine and uronic acid residues (heparin, DS, CS, and HA) are required for FGF23 to activate FGFR1.

Importantly, the activation of FGFR1c was dose dependent for FGF23 when assessed with *N,O*-SH (Fig. 4A). Furthermore, FGF23 activity increased with increasing *N,O*-SH concentrations (1–10 μg/ml). FGF23 activity increased approximately 300% with 1 μg/ml *N,O*-SH ($P < 0.0001$ *vs*. no heparin and no FGF23 controls). This response continued to increase with increasing *N,O*-SH concentrations and plateaued between 8 and 10 μg/ml (Fig. 4B). Importantly, the same set of highly sulfated GAG analogs that promoted activation of FGFR1c by FGF23 also showed similar effects for activation of FGFR2c, 3c, and 4 by FGF23 (not shown).

Effects of degree of heparin polymerization on FGF23 activity

To define the GAG motifs required for FGF23 activity, we used purified heparin oligosaccharide fractions with increasing dp in mitogenic assays. As expected, we obtained a positive correlation between dp and FGF23 activity (Fig. 5). Activation of FGFR1c was significantly increased at dp10 ($P < 0.001$), and at least a doubling of FGF23 activity occurred between dp14 and dp16 ($P < 0.0001$ *vs*. control).

Effects of FGF23 on cellular tyrosine kinase phosphorylation

The FGFs are known to modulate their cellular activities through receptor tyrosine kinase-signaling pathways. Therefore, we examined the effects of FGF23 on total cellular phosphotyrosine in OK cells using an established ELISA. FGF23 (100 nM) significantly increased cellular tyrosine kinase activity to similar extents with or without heparin [89% without *N*,*O*-SH and 107% with *N*,*O*-SH (Fig. 6; $P < 0.0001$ *vs*. control)], indicating that this activity was independent of exogenous fully sulfated *N*,*O*-SH. As control, PTH had no effect on tyrosine kinase phosphorylation in OK cells (Fig. 6) due to the fact that PTH signals through the cAMP and PKC pathways.

FGF23 down-regulates sodium phosphate cotransporter (Npt2a) mRNA in OK cells

When delivered *in vivo*, FGF23 down-regulates the mRNA encoding the kidney proximal tubule sodium-phosphate co-transporter Npt2a, which is primarily responsible for renal reabsorption of phosphate (7, 15–17, 35). To assess the structural requirements of heparin for activity of FGF23 in target cells, we used the OK cell line, which resembles kidney proximal tubule cells and expresses Npt2a. Twenty-four-hour treatment with FGF23 (100 nM) led to down-regulation of Npt2a mRNA by approximately 35%. PTH (100 nM), used as the positive control, had a similar effect (Fig. 7A). Importantly, FGF23 decreased Npt2a mRNA expression to the same degree with or without exogenous fully sulfated *N*,*O*-SH (Fig. 7A), a GAG permissive for FGF23-mediated BaF3 cell mitogenesis (Fig. 3). These data, together with our tyrosine phosphorylation data (Fig. 6), indicate that OK cells express GAGs that support FGF23 activity. To determine whether the expression of cell surface GAGs was required for FGF23 activity, GAGs were removed from OK cells using chlorate treatment (50 mM), as previously described (27, 28). This treatment inhibited the effect of FGF23 on Npt2a mRNA expression, whereas exogenous *N*,*O*-SH restored the ability of FGF23 to down-regulate Npt2a mRNA (Fig. 7B). Furthermore, addition of HS-M, which had no effect on FGF23 activity in proliferation assays (Fig. 3), had no significant effect on FGF23 activity after chlorate treatment (Fig. 7B). PTH was still capable of down-regulating Npt2a mRNA regardless of chlorate treatment (Fig. 7B). Our experiments demonstrate that OK cells express GAGs that are required for FGF23 activity in these cells. Together our data support that FGF23 uses highly sulfated GAGs to act upon specific FGFRs to initiate effects in proximal tubule cells.

Discussion

The identification of the FGFRs activated by FGF23 is critical for understanding the molecular mechanisms involved in the pathogenesis of syndromes associated with dysregulated circulation of this factor, as well as for understanding the role of FGF23 in

normal mineral ion homeostasis and in embryonic development. Herein, we demonstrate that FGF23 interacts with a subset of the seven primary FGFR splicing isoforms, because SPR data and proliferation assays showed that FGF23 bound and activated only the c isoforms of FGFR1-3, as well as FGFR4 (Figs. 1 and 2). The moderate FGF23-FGFR dissociation constants are in the range of dissociation constants we previously measured for other well-characterized FGF-FGFR interactions (20). In this regard, FGF4 and FGF6 bind FGFR1c with dissociation constants of 100–200 nM, and FGF10 binds FGFR2b with an affinity of 622 nM (20, 21). FGF23-FGFR interactions were also analyzed by SPR in an earlier report by Yamashita *et al*. (36), who indicated that FGF23 bound to FGFR3c and 2c. However, FGF23 was reported not bind to FGFR1c, and the FGFR isoforms 1b, 2b, 3b, and 4 were not examined in parallel (36). Additionally, the dissociation constants for FGF23 determined in our present study (Table 2) are 10–40 times higher than in the earlier FGF23 SPR studies [200–700 nM (Table 2) *vs*. 18 nM (36)]. The differences in SPR data between our study and this earlier report could be due to different receptor preparation before SPR analysis because our receptor ectodomains contained no fusion protein tags and were purified in a heparinfree cell system to avoid the presence of GAGs that may artificially increase binding affinity. It is significant that FGF1 activated the FGFRs with greater efficacy than FGF23 (Figs. 2 and 3). This is consistent with available SPR data showing that FGF1 binds FGFR1c, 2c, and 3c with at least 2–7-fold higher affinity than FGF23 (20, 21).

We demonstrated that FGF23 binds and activates multiple FGFR isoforms (Figs. 1 and 2). Taken together with analyses indicating that several FGFRs are expressed within kidney tubule segments and OK cells, our results highlight the possibility that FGFR functional redundancy may exist for FGF23 within the proximal tubule. Indeed, consistent with our results implicating multiple receptors, Fgfr2 and Fgfr3 have been localized specifically to renal proximal tubule cells (37, 38). Furthermore, mRNA encoding Fgfr3b and Fgfr3c were detectable in OK cells, with Fgfr3c as the major isoform (36). These findings were further confirmed by RT-PCR and Western blotting showing that FGFR1-4 were present in OK cells (39), and all seven FGFR splicing isoforms can be detected by RT-PCR in kidney cortex (38). Of note, the recently reported Fgf23-null mice are remarkable for multiple findings in addition to those involved in mineral metabolism, such as hyperphosphatemia and elevated vitamin D levels, and include immature reproductive organs, atrophy of the thymus, low serum triglycerides, elevated serum cholesterol, and hypoglycemia (18, 19). These widespread physiological effects of Fgf23 gene ablation suggest that FGF23 signaling occurs through multiple FGFR isoforms. In addition to its role in phosphate homeostasis, FGF23 regulates vitamin D metabolism. When delivered *in vivo* by injection or in transgenic models, FGF23 down-regulates the vitamin D 1α-hydroxylase enzyme in the proximal tubule (40). Whether distinct FGFR isoforms control phosphate and vitamin D metabolism, or the same FGFR controls both phosphate and vitamin D metabolism, is currently unknown.

Genetic manipulation of mice has not led to an obvious conclusion regarding which of the individual FGFRs may mediate FGF23 actions. Mice null for Fgfr1 and Fgfr2 are embryonic lethal (41), and mice null for Fgfr3 and Fgfr4 do not have an obvious phosphate phenotype (42, 43). Thus, it is possible that FGF23 could signal through multiple FGFRs to regulate

Npt2a and, thus, phosphate homeostasis, and the lack of expression of one Fgfr in animal models may be compensated by expression and activation of a different Fgfr isoform. Corollary to these observations, activating mutations in FGFR1, 2, and 3 are known to give rise to human skeletal disorders involving craniosynostosis and dwarfism (for reviews, see Refs. 44 and 45). The direct association of these skeletal disorders with a phosphate phenotype has not been reported, however. Thus, decreased activity of another FGFR may compensate for the intrinsically active FGFR mutants.

The composition of GAG backbones has a dramatic effect on FGF23 activation, because heparin, CS, DS, and HA groups were permissive for activity (Fig. 3). In addition, heparin oligosaccharides of larger dp provided increased FGF23 activity (Fig. 5), which indicates that larger GAGs may increase the affinity of FGF23 for its receptors. Interestingly, the pathogenesis of XLH can involve enthesopathy or calcification of the tendons and ligaments in the joints (46). Evidence from the Fgf23-null mouse indicates that ablation of Fgf23 results in exostosis-like skeletal formation in the ribcage and extremities, as well as mineralization in soft tissues, suggesting a role for FGF23 in normal cartilage function (18, 19). We were able to demonstrate that CS, which is specifically produced within cartilage, was permissive for FGF23 activity with the FGFRs (Fig. 3). Speculatively, increased activity of FGF23 in the presence of CS within the joints could potentially account for a portion of the inappropriately calcified tissue in severely affected XLH patients.

FGF23 is a regulator of phosphate homeostasis through its inhibitory actions on the sodium-phosphate cotransporter Npt2a, an effect that has been demonstrated *in vivo* after FGF23 delivery to mice (17). It was previously reported that FGFR1-4 were present in OK cells (36, 39). Consistent with this previous study, herein we demonstrated that FGF23 has biological activity in OK cells, as evidenced by inducing tyrosine kinase phosphorylation and down-regulating Npt2a mRNA (Figs. 6 and 7A). Our data demonstrating the characteristics of FGF23 activity in OK cells are consistent with Bowe *et al*. (47), who revealed that FGF23 inhibited sodium-dependent phosphate uptake in OK cell transport assays. Of significance, our data and those of Bowe *et al*. demonstrate that the effects of FGF23 are not dependent upon exogenous heparin. Those data are in contrast to another report suggesting that exogenous heparin/HS is required for FGF23 activity in OK cells (36). Although the exact composition of GAG analogs expressed within the proximal tubule is currently unknown, sulfonated heparin analogs influenced other endocrine systems in cultured rabbit proximal tubule cells, indicating that spatial expression of specific GAGs is critical for normal renal cellular function (48). Notably, multiple sublines of OK cells are available, each of which could express GAGs permissive or nonpermissive for FGF23 action or contain different FGFR numbers or isoforms, depending upon cell culture conditions. Furthermore, lotto-lot differences in the concentration of highly sulfated GAG moieties in commercial preparations of heparin could also be responsible for the apparently disparate FGF23 effects *in vitro*. Our data showing that FGF23 requires highly sulfated GAGs to exert its activity, together with the fact that OK cells naturally express GAGs permissive for FGF23 activity, point to a potential mechanism by which FGF23 may move from bone to the kidney through the circulation without being trapped by HS species present in the extracellular matrix of bone or other nontarget tissues along the path.

In conclusion, the present studies demonstrate that FGF23 binds and activates FGFR1c, 2c, 3c, and 4, stimulates these receptor isoforms in the presence of highly sulfated heparins, and also has activity dependent upon the expression of specific cell-surface GAGs. The isolation of FGFRs that interact with FGF23 could potentially be important for the design of FGF23 antagonists for disorders associated with hypophosphatemia and increased FGF23 activity such as ADHR, XLH, TIO, and fibrous dysplasia, as well as agonists for hyperphosphatemic disorders and decreased FGF23 activity, such as tumoral calcinosis and, perhaps, chronic kidney disease.

Acknowledgments

We are very grateful to Michael J. Econs, M.D., for scientific advice during the course of these studies.

This work was supported by Public Health Service Grant HD39952 (to D.M.O.) and Grants DE13686 (to M.M.), HL052622 and HL062244 (to R.J.L.), and DK063934 (to K.E.W.) from the National Institutes of Health. M.M. is also funded, in part, by a Hirschl Award. We also acknowledge the support of the Indiana Genomics Initiative (INGEN), which is supported, in part, by the Lilly Endowment, Inc.

Abbreviations

ADHR	Autosomal dominant hypophosphatemic rickets
CS	chondroitin sulfate
dp	degree(s) of polymerization
DS	dermatan sulfate
FBS	fetal bovine serum
FGF	fibroblast growth factor
FGFR	fibroblast growth factor receptor
GAG	glycosaminoglycan
HA	hyaluronic acid
HS	heparan sulfate
HS-M	heparin monosulfate
***N,O*-SH**	*N*,*O*-sulfated heparin
***O*-CS**	*O*-sulfated chondroitin sulfate
***O*-DS**	*O*-sulfated dermatan sulfate
***O*-HA**	*O*-sulfated hyaluronic acid
OK	opossum kidney
SPR	surface plasmon resonance
TIO	tumor-induced osteomalacia
XLH	X-linked hypophosphatemia

References

1. Johnson DE, Williams LT. Structural and functional diversity in the FGF receptor multigene family. Adv Cancer Res. 1993; 60:1–41. [PubMed: 8417497]
2. Werner S, Duan DS, de Vries C, Peters KG, Johnson DE, Williams LT. Differential splicing in the extracellular region of fibroblast growth factor receptor 1 generates receptor variants with different ligand-binding specificities. Mol Cell Biol. 1992; 12:82–88. [PubMed: 1309595]
3. Ornitz DM, Xu J, Colvin JS, McEwen DG, MacArthur CA, Coulier F, Gao G, Goldfarb M. Receptor specificity of the fibroblast growth factor family. J Biol Chem. 1996; 271:15292–15297. [PubMed: 8663044]
4. Allen BL, Rapraeger AC. Spatial and temporal expression of heparan sulfate in mouse development regulates FGF and FGF receptor assembly. J Cell Biol. 2003; 163:637–648. [PubMed: 14610064]
5. The ADHR Consortium. Autosomal dominant hypophosphataemic rickets is associated with mutations in FGF23. Nat Genet. 2000; 26:345–348. [PubMed: 11062477]
6. White KE, Carn G, Lorenz-Depiereux B, Benet-Pages A, Strom TM, Econs MJ. Autosomal-dominant hypophosphatemic rickets (ADHR) mutations stabilize FGF-23. Kidney Int. 2001; 60:2079–2086. [PubMed: 11737582]
7. Liu S, Guo R, Simpson LG, Xiao ZS, Burnham CE, Quarles LD. Regulation of fibroblastic growth factor 23 expression but not degradation by PHEX. J Biol Chem. 2003; 278:37419–37426. [PubMed: 12874285]
8. Jonsson KB, Zahradnik R, Larsson T, White KE, Sugimoto T, Imanishi Y, Yamamoto T, Hampson G, Koshiyama H, Ljunggren O, Oba K, Yang IM, Miyauchi A, Econs MJ, Lavigne J, Juppner H. Fibroblast growth factor 23 in oncogenic osteomalacia and X-linked hypophosphatemia. N Engl J Med. 2003; 348:1656–1663. [PubMed: 12711740]
9. Yamazaki Y, Okazaki R, Shibata M, Hasegawa Y, Satoh K, Tajima T, Takeuchi Y, Fujita T, Nakahara K, Yamashita T, Fukumoto S. Increased circulatory level of biologically active full-length FGF-23 in patients with hypophosphatemic rickets/osteomalacia. J Clin Endocrinol Metab. 2002; 87:4957–4960. [PubMed: 12414858]
10. Riminucci M, Collins MT, Fedarko NS, Cherman N, Corsi A, White KE, Waguespack S, Gupta A, Hannon T, Econs MJ, Bianco P, Gehron Robey P. FGF-23 in fibrous dysplasia of bone and its relationship to renal phosphate wasting. J Clin Invest. 2003; 112:683–692. [PubMed: 12952917]
11. Benet-Pages A, Orlik P, Strom TM, Lorenz-Depiereux B. An FGF23 missense mutation causes familial tumoral calcinosis with hyperphosphatemia. Hum Mol Genet. 2005; 14:385–390. [PubMed: 15590700]
12. Larsson T, Yu X, Davis SI, Draman MS, Mooney SD, Cullen MJ, White KE. A novel recessive mutation in Fibroblast growth factor-23 (FGF23) causes familial tumoral calcinosis. J Clin Endocrinol Metab. 2005; 90:2424–2427. [PubMed: 15687325]
13. Ferrari SL, Bonjour JP, Rizzoli R. FGF-23 relationship to dietary phosphate and renal phosphate handling in healthy young men. J Clin Endocrinol Metab. 2005; 90:1519–1524. [PubMed: 15613425]
14. Bai X, Miao D, Li J, Goltzman D, Karaplis AC. Transgenic mice overexpressing human fibroblast growth factor 23 (R176Q) delineate a putative role for parathyroid hormone in renal phosphate wasting disorders. Endocrinology. 2004; 145:5269–5279. [PubMed: 15284207]
15. Shimada T, Urakawa I, Yamazaki Y, Hasegawa H, Hino R, Yoneya T, Takeuchi Y, Fujita T, Fukumoto S, Yamashita T. FGF-23 transgenic mice demonstrate hypophosphatemic rickets with reduced expression of sodium phosphate cotransporter type IIa. Biochem Biophys Res Commun. 2004; 314:409–414. [PubMed: 14733920]
16. Larsson T, Marsell R, Schipani E, Ohlsson C, Ljunggren O, Tenenhouse HS, Juppner H, Jonsson KB. Transgenic mice expressing Fibroblast Growth Factor 23 under the control of the α1(I) collagen promoter exhibit growth retardation, osteomalacia and disturbed phosphate homeostasis. Endocrinology. 2004; 145:3087–3094. [PubMed: 14988389]
17. Shimada T, Hasegawa H, Yamazaki Y, Muto T, Hino R, Takeuchi Y, Fujita T, Nakahara K, Fukumoto S, Yamashita T. FGF-23 is a potent regulator of vitamin D metabolism and phosphate homeostasis. J Bone Miner Res. 2004; 19:429–435. [PubMed: 15040831]

18. Shimada T, Kakitani M, Yamazaki Y, Hasegawa H, Takeuchi Y, Fujita T, Fukumoto S, Tomizuka K, Yamashita T. Targeted ablation of Fgf23 demonstrates an essential physiological role of FGF23 in phosphate and vitamin D metabolism. J Clin Invest. 2004; 113:561–568. [PubMed: 14966565]
19. Sitara D, Razzaque MS, Hesse M, Yoganathan S, Taguchi T, Erben RG, J Apw-Ppner H, Lanske B. Homozygous ablation of fibroblast growth factor-23 results in hyperphosphatemia and impaired skeletogenesis, and reverses hypophosphatemia in Phex-deficient mice. Matrix Biol. 2004; 23:421–432. [PubMed: 15579309]
20. Ibrahimi OA, Zhang F, Eliseenkova AV, Linhardt RJ, Mohammadi M. Proline to arginine mutations in FGF receptors 1 and 3 result in Pfeiffer and Muenke craniosynostosis syndromes through enhancement of FGF binding affinity. Hum Mol Genet. 2004; 13:69–78. [PubMed: 14613973]
21. Ibrahimi OA, Zhang F, Eliseenkova AV, Itoh N, Linhardt RJ, Mohammadi M. Biochemical analysis of pathogenic ligand-dependent FGFR2 mutations suggests distinct pathophysiological mechanisms for craniofacial and limb abnormalities. Hum Mol Genet. 2004; 13:2313–2324. [PubMed: 15282208]
22. Maruyama T, Toida T, Imanari T, Yu G, Linhardt RJ. Conformational changes and anticoagulant activity of chondroitin sulfate following its O-sulfonation. Carbohydr Res. 1998; 306:35–43. [PubMed: 9691438]
23. Toida T, Maruyama T, Ogita Y, Suzuki A, Toyoda H, Imanari T, Linhardt RJ. Preparation and anticoagulant activity of fully O-sulphonated glycosaminoglycans. Int J Biol Macromol. 1999; 26:233–241. [PubMed: 10569284]
24. Garg HG, Joseph PA, Thompson BT, Hales CA, Toida T, Imanari T, Capila I, Linhardt RJ. Effect of fully sulfated glycosaminoglycans on pulmonary artery smooth muscle cell proliferation. Arch Biochem Biophys. 1999; 371:228–233. [PubMed: 10545209]
25. Linhardt RJ, Rice KG, Kim YS, Engelken JD, Weiler JM. Homogeneous, structurally defined heparin-oligosaccharides with low anticoagulant activity inhibit the generation of the amplification pathway C3 convertase in vitro. J Biol Chem. 1988; 263:13090–13096. [PubMed: 3417651]
26. Pervin A, Gallo C, Jandik KA, Han XJ, Linhardt RJ. Preparation and structural characterization of large heparin-derived oligosaccharides. Glycobiology. 1995; 5:83–95. [PubMed: 7772871]
27. Humphries DE, Silbert JE. Chlorate: a reversible inhibitor of proteoglycan sulfation. Biochem Biophys Res Commun. 1988; 154:365–371. [PubMed: 2969240]
28. Safaiyan F, Kolset SO, Prydz K, Gottfridsson E, Lindahl U, Salmivirta M. Selective effects of sodium chlorate treatment on the sulfation of heparan sulfate. J Biol Chem. 1999; 274:36267–36273. [PubMed: 10593915]
29. Livak KJ, Schmittgen TD. Analysis of relative gene expression data using real-time quantitative PCR and the 2(-Delta Delta C(T)) Method. Methods. 2001; 25:402–408. [PubMed: 11846609]
30. Ornitz DM, Yayon A, Flanagan JG, Svahn CM, Levi E, Leder P. Heparin is required for cell-free binding of basic fibroblast growth factor to a soluble receptor and for mitogenesis in whole cells. Mol Cell Biol. 1992; 12:240–247. [PubMed: 1309590]
31. Collins MK, Downward J, Miyajima A, Maruyama K, Arai K, Mulligan RC. Transfer of functional EGF receptors to an IL3-dependent cell line. J Cell Physiol. 1988; 137:293–298. [PubMed: 3263970]
32. D'Andrea AD, Yoshimura A, Youssoufian H, Zon LI, Koo JW, Lodish HF. The cytoplasmic region of the erythropoietin receptor contains nonoverlapping positive and negative growth-regulatory domains. Mol Cell Biol. 1991; 11:1980–1987. [PubMed: 1848667]
33. Hatakeyama M, Mori H, Doi T, Taniguchi T. A restricted cytoplasmic region of IL-2 receptor β chain is essential for growth signal transduction but not for ligand binding and internalization. Cell. 1989; 59:837–845. [PubMed: 2590941]
34. Wang JK, Gao G, Goldfarb M. Fibroblast growth factor receptors have different signaling and mitogenic potentials. Mol Cell Biol. 1994; 14:181–188. [PubMed: 8264585]
35. Bai XY, Miao D, Goltzman D, Karaplis AC. The autosomal dominant hypophosphatemic rickets R176Q mutation in fibroblast growth factor 23 resists proteolytic cleavage and enhances in vivo biological potency. J Biol Chem. 2003; 278:9843–9849. [PubMed: 12519781]

36. Yamashita T, Konishi M, Miyake A, Inui K, Itoh N. Fibroblast growth factor (FGF)-23 inhibits renal phosphate reabsorption by activation of the mitogen-activated protein kinase pathway. J Biol Chem. 2002; 277:28265–28270. [PubMed: 12032146]
37. Cancilla B, Ford-Perriss MD, Bertram JF. Expression and localization of fibroblast growth factors and fibroblast growth factor receptors in the developing rat kidney. Kidney Int. 1999; 56:2025–2039. [PubMed: 10594778]
38. Cancilla B, Davies A, Cauchi JA, Risbridger GP, Bertram JF. Fibroblast growth factor receptors and their ligands in the adult rat kidney. Kidney Int. 2001; 60:147–155. [PubMed: 11422746]
39. Yan X, Yokote H, Jing X, Yao L, Sawada T, Zhang Y, Liang S, Sakaguchi K. Fibroblast growth factor 23 reduces expression of type IIa Na+/Pi co-transporter by signaling through a receptor functionally distinct from the known FGFRs in opossum kidney cells. Genes Cells. 2005; 10:489–502. [PubMed: 15836777]
40. Shimada T, Mizutani S, Muto T, Yoneya T, Hino R, Takeda S, Takeuchi Y, Fujita T, Fukumoto S, Yamashita T. Cloning and characterization of FGF23 as a causative factor of tumor-induced osteomalacia. Proc Natl Acad Sci USA. 2001; 98:6500–6505. [PubMed: 11344269]
41. Deng CX, Wynshaw-Boris A, Shen MM, Daugherty C, Ornitz DM, Leder P. Murine FGFR-1 is required for early postimplantation growth and axial organization. Genes Dev. 1994; 8:3045–3057. [PubMed: 8001823]
42. Deng C, Wynshaw-Boris A, Zhou F, Kuo A, Leder P. Fibroblast growth factor receptor 3 is a negative regulator of bone growth. Cell. 1996; 84:911–921. [PubMed: 8601314]
43. Yu K, Xu J, Liu Z, Sosic D, Shao J, Olson EN, Towler DA, Ornitz DM. Conditional inactivation of FGF receptor 2 reveals an essential role for FGF signaling in the regulation of osteoblast function and bone growth. Development. 2003; 130:3063–3074. [PubMed: 12756187]
44. Ornitz DM, Marie PJ. FGF signaling pathways in endochondral and intramembranous bone development and human genetic disease. Genes Dev. 2002; 16:1446–1465. [PubMed: 12080084]
45. Wilkie AO, Patey SJ, Kan SH, van den Ouweland AM, Hamel BC. FGFs, their receptors, and human limb malformations: clinical and molecular correlations. Am J Med Genet. 2002; 112:266–278. [PubMed: 12357470]
46. Tenenhouse, HS.; Econs, MJ. Mendelian hypophosphatemias. In: Scriver CR ed. The metabolic and molecular basis of inherited disease. 8th ed. New York: McGraw-Hill; 2001. p. 5039-5067.
47. Bowe AE, Finnegan R, Jan de Beur SM, Cho J, Levine MA, Kumar R, Schiavi SC. FGF-23 inhibits renal tubular phosphate transport and is a PHEX substrate. Biochem Biophys Res Commun. 2001; 284:977–981. [PubMed: 11409890]
48. Yard BA, Chorianopoulos E, Herr D, van der Woude FJ. Regulation of endothelin-1 and transforming growth factor-β1 production in cultured proximal tubular cells by albumin and heparan sulphate glycosaminoglycans. Nephrol Dial Transplant. 2001; 16:1769–1775. [PubMed: 11522857]

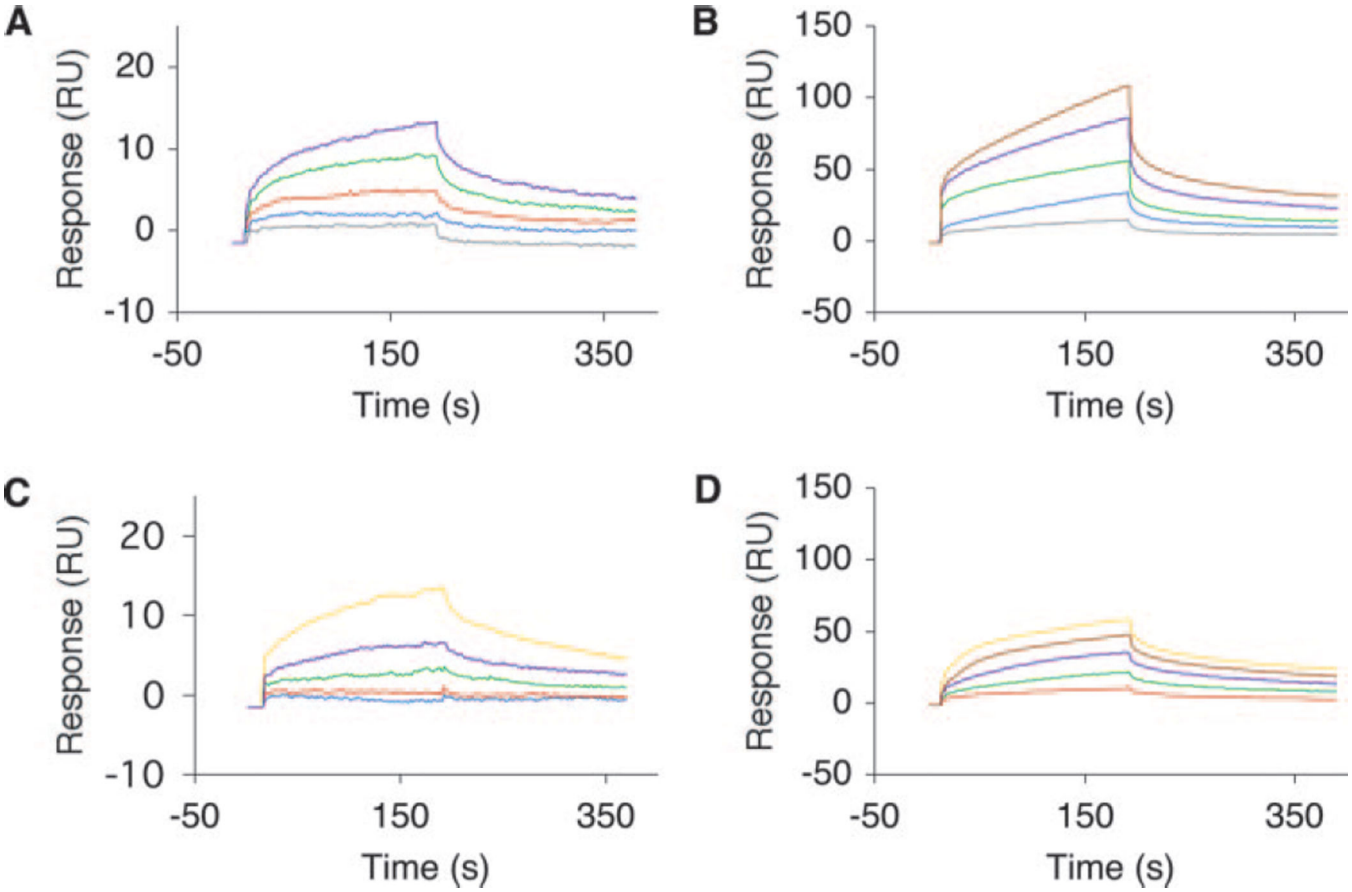

Fig. 1.

Analysis of FGF23-FGFR binding by SPR. SPR sensorgrams illustrating FGF23 binding to FGFR1c (A), FGFR2c (B), FGFR3c (C), and FGFR4 (D). Analyte concentrations are colored as follows: 25 nM in *gray*, 50 nM in *blue*, 100 nM in *red*, 200 nM in *green*, 400 nM in *violet*, 800 nM in *brown*, and 1000 nM in *gold*. The biosensor chip response is indicated on the y-axis (RU) as a function of time (x-axis). Binding experiments were performed at 25 C.

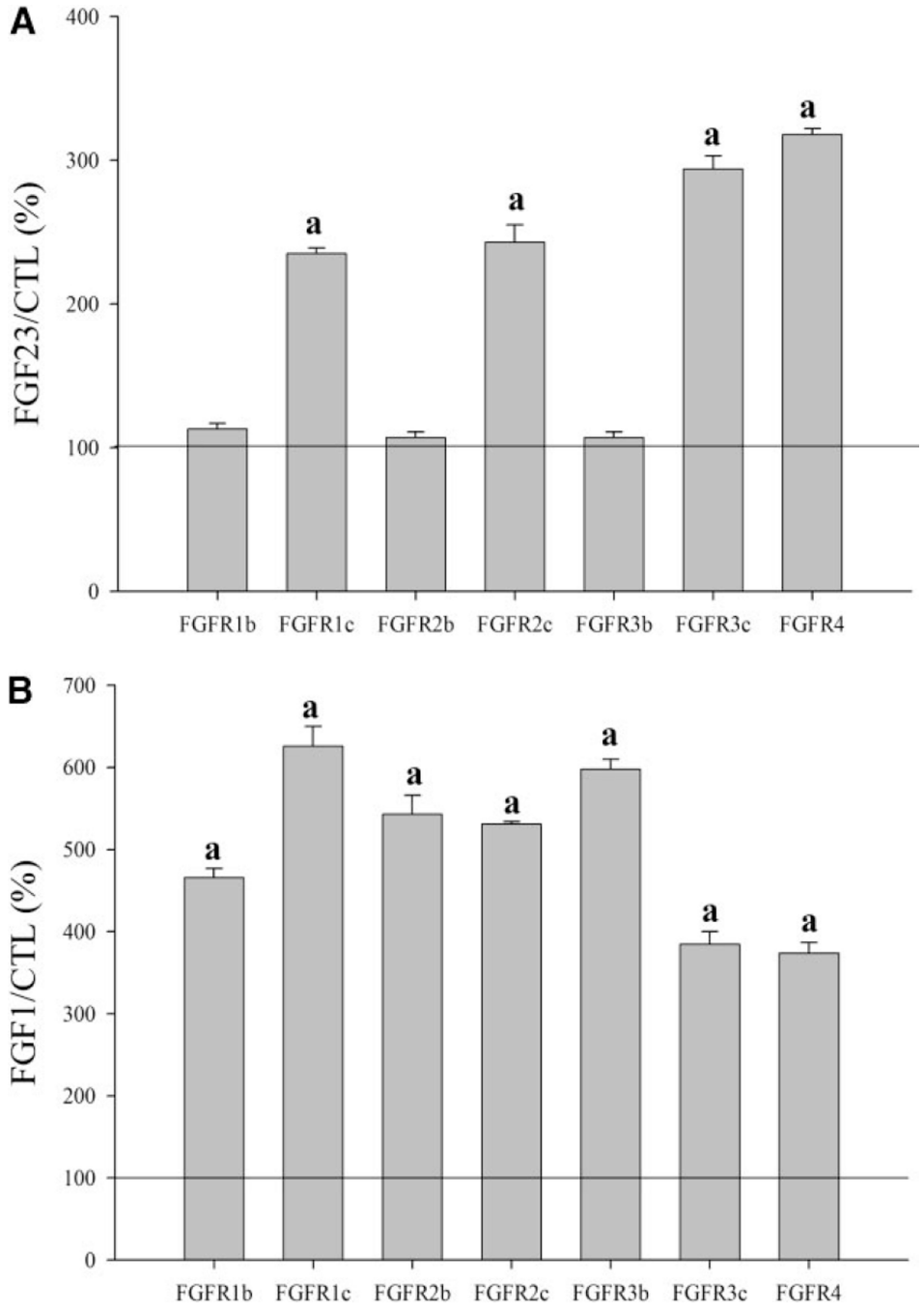

Fig. 2.

Activation of FGFRs by FGF23 assessed by cell proliferation. A, BaF3 cell lines each expressing one of the FGFR subtypes (FGFR1b, 1c, 2b, 2c, 3b, 3c, and 4) were treated with FGF23 (100 nM) and a preparation of unbleached heparin (2 μg/ml). FGF23 activated the c isoforms of FGFR1-3 and FGFR4. It showed negligible activity toward the b isoforms of FGFR1-3. B, FGF1 (5 nM) activated all FGFR isoforms. The results are plotted as percentage of control (no treatment) for each cell line. *a*, $P < 0.05$ *vs*. control (CTL).

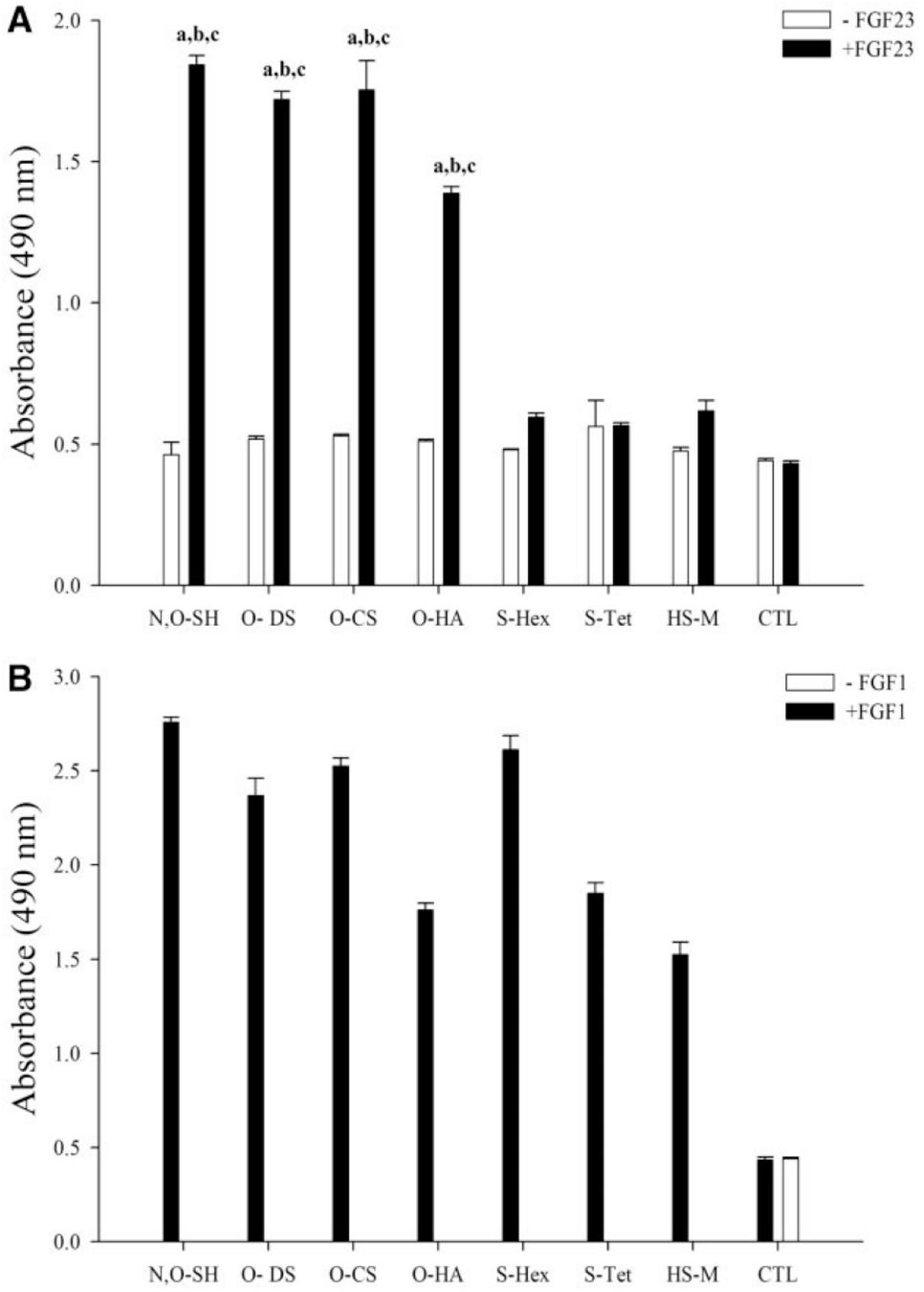

Fig. 3.

Activation of FGFR1c by FGF23 in the presence of sulfated GAGs. A, BaF3 cells expressing FGFR1c were treated with FGF23 (100 nM) with or without addition of heparin (2 μg/ml). The mitogenic activity of FGF23 was significantly increased by fully sulfated *N*, *O*-SH, *O*-DS, *O*-CS, and *O*-HA. In contrast, highly sulfated polysaccharides, as well as HS-M, did not synergize with FGF23 [*a*, $P < 0.001$ *vs*. CTL; *b*, $P < 0.001$ *vs*. FGF23 alone; *c*, $P < 0.001$ *vs*. respective heparin derivative alone]. B, FGF1 (5 nM) activated FGFR1c

regardless of the sugar backbone of the GAG ($P < 0.0001$, *vs*. CTL, FGF1 alone, and respective heparin derivative alone).

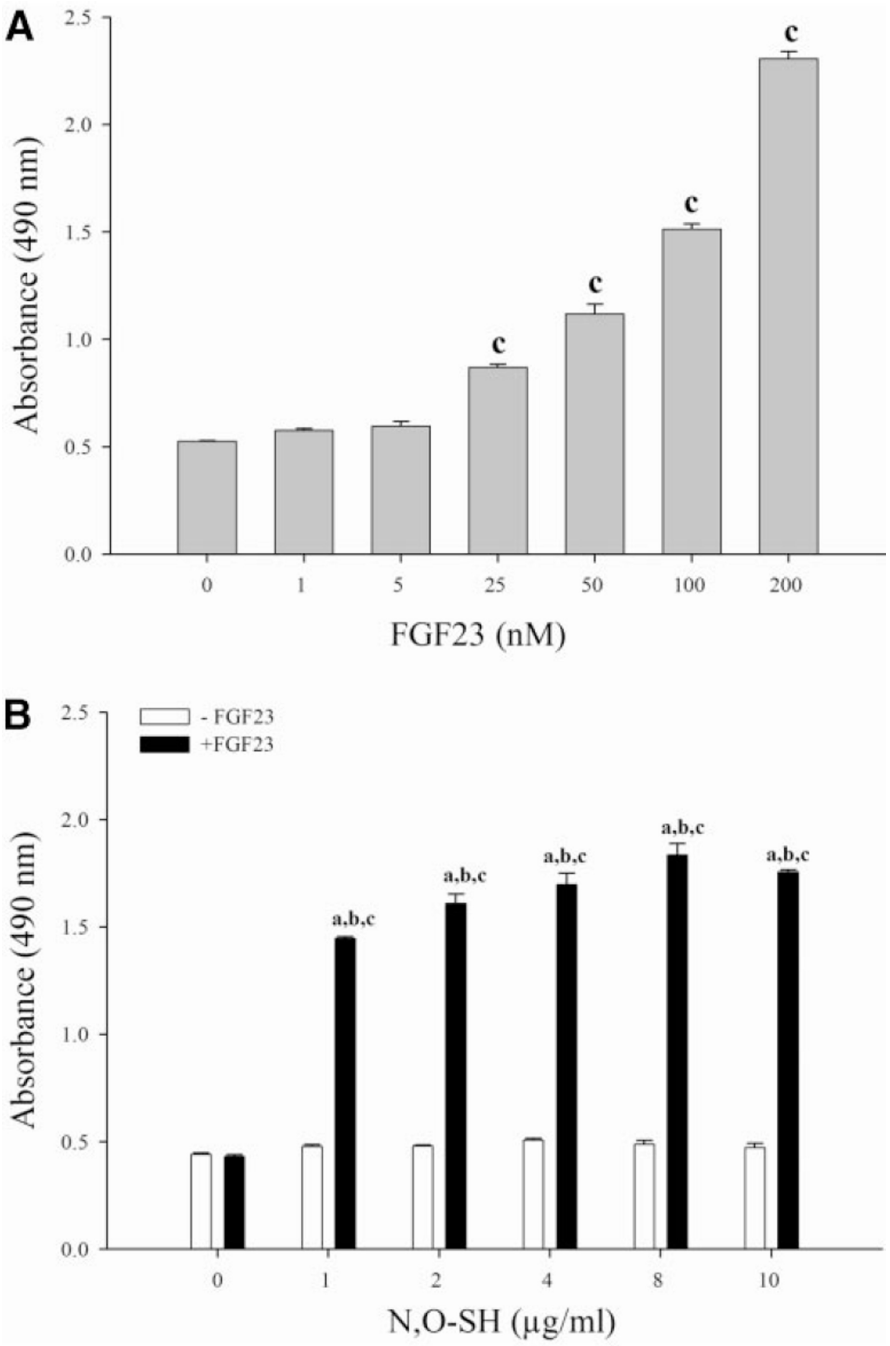

Fig. 4.

Dose dependence of FGFR1c activation by FGF23 and *N*, *O*-SH. A, BaF3 cells expressing FGFR1c were treated with increasing doses of FGF23 in the presence of 2 µg/ml *N*, *O*-SH. Mitogenic activity of FGF23 showed dose dependence, with a threshold dose of approximately 25 nM and an ED_{50} of approximately 50 nM (*c*, $P < 0.0001$ *vs.* *N*, *O*-SH alone). B, Increasing doses of *N*, *O*-SH resulted in increasing activity of FGF23 [a, $P < 0.001$ *vs*. control (CTL); b, $P < 0.001$ *vs*. FGF23 alone; c, $P < 0.001$ *vs*. heparin alone].

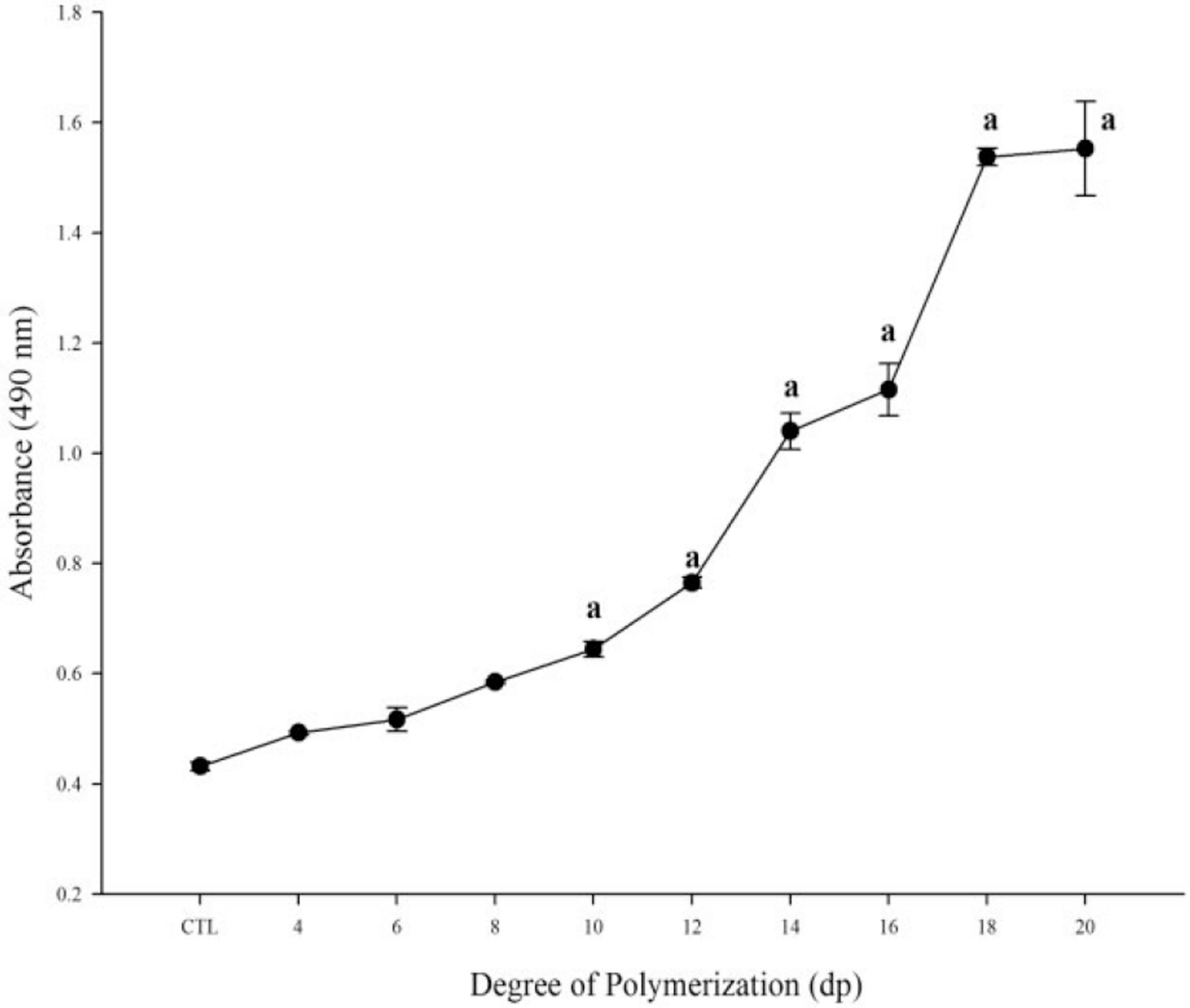

Fig. 5.

FGF23 activity correlates with dp of heparin. BaF3 cells expressing FGFR1c were treated with FGF23 (100 nM) and heparins with increasing dp. Synergism of heparins with FGF23 became evidence at dp10 [$P < 0.001$ *vs*. control (CTL), treatment with dp20 alone]. A doubling of FGF23 activity was observed with heparins of dp in the range of 14–16 ($P < 0.0001$ *vs*. control).

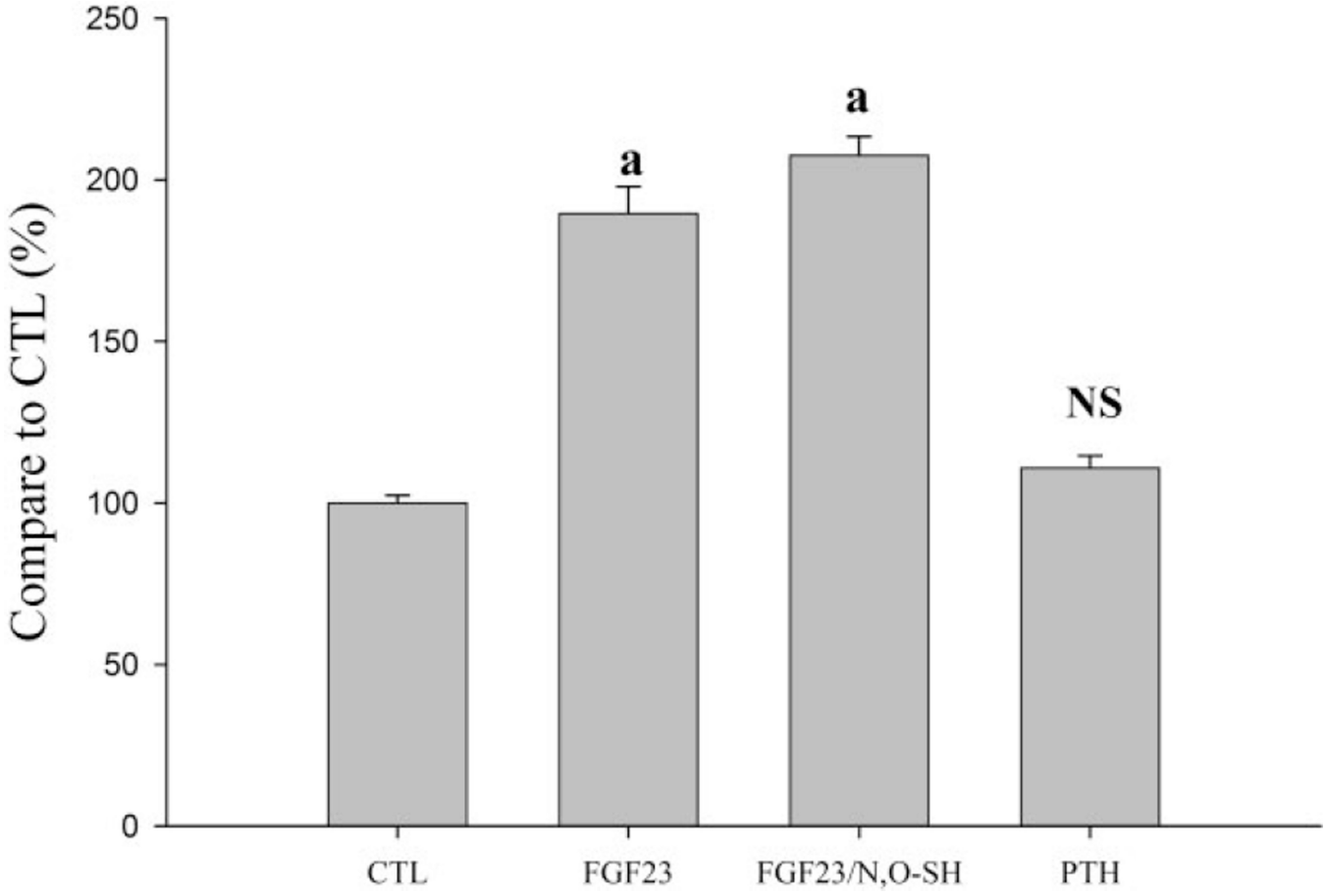

Fig. 6.

Effect of FGF23 on cellular tyrosine kinase phosphorylation. OK cells were treated for 15 min with either vehicle (CTL), PTH (100 nM), or FGF23 (100 nM) with or without 2 μg/ml *N,O-SH*, and the effects on cellular tyrosine kinase phosphorylation were examined by ELISA. FGF23 significantly increased cellular tyrosine kinase independently of exogenous fully sulfonated *N*, *O*-SH [$P < 0.0001$ *vs*. control (CTL)]. As expected, PTH had no effect on tyrosine kinase phosphorylation in OK cells. Data shown compared with vehicle control (*a*, $P < 0.0001$ *vs*. control). NS, not significant.

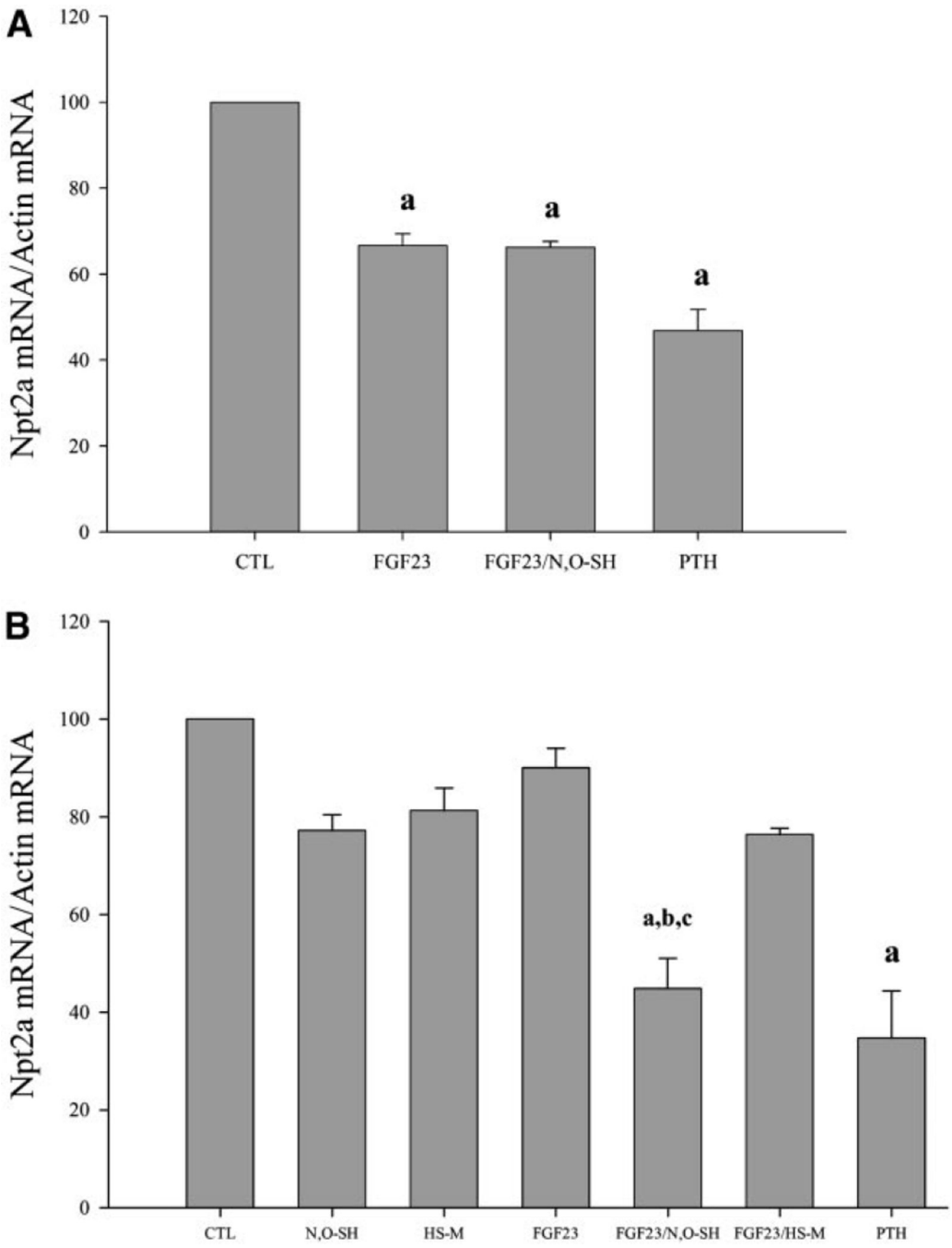

Fig. 7.

Effect of FGF23 on NPT2a mRNA expression. A, OK cells were treated over 24 h with either vehicle (CTL), PTH (100 nM), or FGF23 (100 nM) with or without 2 μg/ml *N,O-SH*, and the effects on Npt2a mRNA were examined. FGF23 robustly decreased Npt2a mRNA expression, and its effect did not require *N*, *O*-SH [$P < 0.001$ *vs*. control (CTL)]. PTH, included as a positive control, had a similar effect. B, OK cells were treated with sodium chlorate (50 mM) to block sulfation of GAGs. PTH or FGF23 was added with or without 2 μg/ml *N*, *O*-SH or HS-M. In this condition, the effect of FGF23 on Npt2a mRNA became

sensitive to exogenous*N*, *O*-SH. *a*, $P < 0.05$ *vs*. CTL; *b*, $P < 0.05$ *vs*. FGF23 alone; *c*,$P < 0.05$ *vs*. heparin alone.

TABLE 1

Primer and probe sequences for real-time quantitative RT-PCR

	Opossum Npt2a (5'–3')	**Opossum β-actin (5'-3')**
Forward	TCACTCGACTCATTATCCAGTTGG	TACAATGAGCTGCGTGTGGC
Reverse	GCTGTGGTTTCGAAGGGTCTC	GGGTTCAAGGGAGCTTCTGTG
Probe	TGATCAATAGCATCGCCACGGGAGA	CCTGAGGAACACCCCGTGCTGC
GenBank accession no.	L26308	AY944136

TABLE 2

Summary of kinetic data of FGF23 interactions with FGFR1-4

FGFR	FGF23
FGFR1c	
K_{on} (/M × sec)[a]	8.31×10^{3}
K_{off} (/sec)[a]	6.08×10^{-3}
K_D (M)[b]	7.32×10^{-7}
FGFR2c	
K_{on} (/M × sec)	1.42×10^{4}
K_{off} (/sec)	3.14×10^{-3}
K_D (M)	2.22×10^{-7}
FGFR3c	
K_{on} (/M × sec)	6.99×10^{3}
K_{off} (/sec)	3.55×10^{-3}
K_D (M)	5.07×10^{-7}
FGFR4	
K_{on} (/M × sec)	1.58×10^{4}
K_{off} (/sec)	4.25×10^{-3}
K_D (M)	2.69×10^{-7}

[a] K_{on} and K_{off} were derived as described in *Materials and Methods*. χ^2 was less than 10% of R_{max} in all cases.

[b] The apparent affinity, K_D, is equal to K_{off}/K_{on}.